AIP Applied Physics Letters

Simultaneous extraction of charge density dependent mobility and variable contact resistance from thin film transistors

Riccardo Di Pietro, Deepak Venkateshvaran, Andreas Klug, Emil J. W. List-Kratochvil, Antonio Facchetti, Henning Sirringhaus, and Dieter Neher

Citation: Applied Physics Letters **104**, 193501 (2014); doi: 10.1063/1.4876057
View online: http://dx.doi.org/10.1063/1.4876057
View Table of Contents: http://scitation.aip.org/content/aip/journal/apl/104/19?ver=pdfcov
Published by the AIP Publishing

Articles you may be interested in

Impact of universal mobility law on polycrystalline organic thin-film transistors
J. Appl. Phys. **112**, 084503 (2012); 10.1063/1.4758182

Mobility saturation in tapered edge bottom contact copper phthalocyanine thin film transistors
J. Vac. Sci. Technol. B **28**, C5F22 (2010); 10.1116/1.3464771

Dependence of field-effect mobility and contact resistance on nanostructure in regioregular poly(3-hexylthiophene) thin film transistors
Appl. Phys. Lett. **92**, 263303 (2008); 10.1063/1.2955515

Modeling of organic thin film transistors: Effect of contact resistances
J. Appl. Phys. **101**, 014501 (2007); 10.1063/1.2402349

Film and contact resistance in pentacene thin-film transistors: Dependence on film thickness, electrode geometry, and correlation with hole mobility
J. Appl. Phys. **99**, 094504 (2006); 10.1063/1.2197033

AIP Journal of Applied Physics

Journal of Applied Physics is pleased to announce André Anders as its new Editor-in-Chief

This article is copyrighted as indicated in the article. Reuse of AIP content is subject to the terms at: http://scitation.aip.org/termsconditions. Downloaded to IP: 141.89.117.114 On: Thu, 17 Jul 2014 14:35:01

Simultaneous extraction of charge density dependent mobility and variable contact resistance from thin film transistors

Riccardo Di Pietro,[1,a)] Deepak Venkateshvaran,[2] Andreas Klug,[3]
Emil J. W. List-Kratochvil,[3,4] Antonio Facchetti,[5] Henning Sirringhaus,[2] and Dieter Neher[1]
[1]*Institut für Physik und Astronomie, Universität Potsdam, Karl-Liebknecht-Str. 24-25, 14476 Potsdam, Germany*
[2]*Cavendish Laboratory, Cambridge University, J. J. Thomson Avenue, CB3 0HE Cambridge, United Kingdom*
[3]*NanoTecCenter Weiz Forschungsgesellschaft mbH, Franz-Pichler-Straße 32, A-8160 Weiz, Austria*
[4]*Institute of Solid State Physics, Graz University of Technology, Petersgasse 32, A-8010 Graz, Austria*
[5]*Polyera Corporation, 8045 Lamon Ave, STE 140, Skokie, Illinois 60077-5318, USA*

(Received 28 January 2014; accepted 30 April 2014; published online 12 May 2014)

A model for the extraction of the charge density dependent mobility and variable contact resistance in thin film transistors is proposed by performing a full derivation of the current-voltage characteristics both in the linear and saturation regime of operation. The calculated values are validated against the ones obtained from direct experimental methods. This approach allows unambiguous determination of gate voltage dependent contact and channel resistance from the analysis of a single device. It solves the inconsistencies in the commonly accepted mobility extraction methods and provides additional possibilities for the analysis of the injection and transport processes in semiconducting materials. © *2014 AIP Publishing LLC*.
[http://dx.doi.org/10.1063/1.4876057]

Field-effect transistors (FETs) are one of the most widely used tools for the analysis of the charge transport properties of semiconducting materials.[1,2] While the working principle is well understood and characterized,[3] there is still no general analytical solution for the current voltage characteristics in presence of charge density dependent mobility,[4] but only limited solutions for a specific functional dependence of mobility on gate voltage.[5–8] The different effects of non-constant mobility in the linear and saturation regime of operation usually lead to different values for mobility extracted in the different regimes.[9] To complicate matters even further, mobility extraction is also hindered by the presence of contact resistance, which is as well dependent on the regime of operation of the transistor[10,11] and leads to artifacts in the mobility extraction procedure.

In order to disentangle the effects of charge density dependent mobility and contact resistance, several techniques have been developed[12] from adaptations of the transmission line method (TLM)[13–19] to more complex techniques such as four point probe (FPP) measurements[20–22] and scanning Kelvin probe microscopy (SKPM).[23,24] Although these techniques allow for a direct measurement of the two parameters, they either involve the comparison of multiple devices (TLM) or are limited to a specific device structure (FPP and SKPM), thus restricting their applicability only to a subset of possible device architectures. To bridge this gap, several analytical models have been proposed to extract the effects of contact resistance from the analysis of the electrical characteristics of working devices.[5,9,25–28] However, the analytical description is complicated by the fact that both mobility and contact resistance are usually both gate voltage dependent, and all the method proposed so far for mobility extraction either assume a constant contact resistance or they still require the comparison of devices with different channel lengths in order to separate the influence of the gate voltage on the two parameters.[27] The role of gate voltage dependent contact resistance is examined in Ref. 9; however, the equations are derived in the case of constant mobility.

In this letter, we report a derivation of the standard current-voltage equation for field-effect transistors[3] including from the beginning a charge density dependent mobility $\mu(V)$ and variable contact resistance, without the need to assume any *a priori* functional dependence of the two parameters on the applied voltages. We show how the explicit inclusion of $\mu(V)$ introduces an additional correction factor in the extraction of the mobility from the saturation regime. A simple method to take into account this correction is proposed, and the obtained mobility is then used to accurately estimate the gate voltage dependent contact resistance for any given device geometry from the analysis of the linear transfer characteristics. By comparing the obtained values with experimental results obtained from gated FPP and gated TLM measurements, one finds that in all cases, the calculated contact resistance and mobility agree both in magnitude and in charge density dependence with those results. The gained flexibility (only the standard saturation and linear transfer characteristics need to be acquired) is demonstrated in the analysis of the influence of organic semiconductor thickness and processing conditions on contact resistivity.

Figure 1 shows a schematic of a field-effect transistor together with the equivalent circuit and all the relevant parameters used in the text. The transistor is operated in a common source configuration ($V_S = 0\,\mathrm{V}$). In the following derivation, each potential is written either as V_X, the potential at position X with respect to the ground, or V_{XY}, the potential difference between two points X and Y, with the exception of $V(x)$ which represents the potential along the channel referred to ground. The derivation is performed for simplicity

[a)]dipietro@uni-potsdam.de

 © 2014 AIP Publishing LLC

This article is copyrighted as indicated in the article. Reuse of AIP content is subject to the terms at: http://scitation.aip.org/termsconditions. Downloaded to IP: 141.89.117.114 On: Thu, 17 Jul 2014 14:35:01

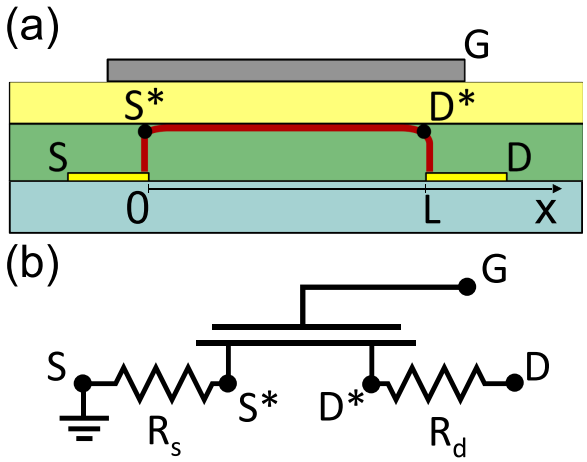

FIG. 1. (a) Schematic cross-section of a bottom-contact top-gate transistor and (b) equivalent circuit of the transistor used to include the effect of source (R_S) and drain (R_D) resistance (gate voltage dependent). The different elements of the circuit represent different parts of the real device, with the points at which the voltage is evaluated marked in both schemes.

considering the onset voltage V_{on} for charge accumulation equal to 0, but the results can be easily extended to the general case without modification, by substituting V_G with $\hat{V}_G = V_G - V_{on}$. The full mathematical derivation is reported in the supplementary material.[29]

The charge sheet model together with the gradual channel approximation[30] allows the charge density per unit area q at position x along the channel to be defined as

$$q(V_G - V(x)) = C_i \cdot (V_G - V(x)), \tag{1}$$

where C_i is the geometric capacitance per unit area in the accumulation regime $\left(|V_G| \geq |V(x)|\right)$. As usually observed in organic and oxide semiconductors, field-effect mobility is dependent on charge density. In order to account for this, we introduce an effective mobility $\mu_{eff}(V)$, defined as the average of the charge density dependent mobility $\mu(v)$ over the charge accumulated at point x for a given voltage difference $V_G - V(x)$ across the dielectric layer

$$\mu_{eff}(V_G - V(x)) = \frac{\int_0^q \mu(\rho)d\rho}{q} = \frac{\int_0^{(V_G - V(x))} \mu(v)dv}{(V_G - V(x))}. \tag{2}$$

Note that μ is an explicit function of the local charge carrier density q, but because of the strictly linear dependence of q on the voltage drop across the insulator (Eq. (1)), it is always written as $\mu(v)$ throughout the following analysis.

Using the effective mobility to calculate the drift current in the transistor channel, the current voltage equation is obtained

$$I = \frac{W}{L} C_i \int_{V_{S^*}}^{V_{D^*}} \left(\int_0^{(V_G - V(x))} \mu(v)dv \right) dV(x), \tag{3}$$

where W and L are the width and length of the transistor's channel and V_{S^*} and V_{D^*} (the effective source and drain potentials) are left unknown.

We first focus on how $\mu(v)$ affects the analysis of the saturation transfer characteristics. In the saturation regime, it is safe to assume $V_{D^*} = V_G$ due to the channel being pinched-off close to the drain electrode. The charge density dependent mobility can be obtained starting from Eq. (3), by evaluating $\left(\frac{d\sqrt{I}}{dV_G}\right)^2$ with the help of a Taylor expansion of $\int_0^{(V_G - V(x))} \mu(v)dv$. We assume that the increase of the voltage drop due to source resistance with the applied gate voltage is limited

$$\frac{dV_{S^*}}{dV_G} \ll 1. \tag{4}$$

SKPM measurements performed in the saturation regime[31,32] show that condition (4) is usually fulfilled, due to the higher resistance of the channel in the saturation regime of operation. By including a charge density dependent mobility, an additional correction factor $k(V_G)$ is introduced in the equation for the mobility extraction (supplementary material, Sec. 1, Ref. 29)

$$\left(\frac{d\sqrt{I}}{dV_G}\right)^2 = \frac{W}{2L} C_i \mu(V_G) \cdot k(V_G). \tag{5}$$

The correction factor is in general not constant and dependent on the particular shape of $\mu(V_G)$. It is easy to show how for $\mu(V_G) = \alpha(V_G)^\beta$ (power laws are usually employed to approximate charge density dependent mobility in organic FETs[5,27]) Eq. (5) becomes (supplementary material, Sec. 2, Ref. 29)

$$\left(\frac{d\sqrt{I}}{dV_G}\right)^2 = \frac{W}{2L} C_i \mu(V_G) \frac{(\beta + 2)}{2(\beta + 1)}, \tag{6}$$

with a gate voltage independent correction factor equal to

$$k = \frac{\beta + 2}{2(\beta + 1)}. \tag{7}$$

For positive values of β (mobility increasing with charge density[4,33]), k will be limited between 1 ($\beta = 0$) and 0.5 ($\beta \to \infty$). As it is always possible to approximate the gate voltage dependence of the mobility in the form of a polynomial function, for any monotonically increasing function, the following inequality holds true:

$$0.5 \leq k(V_G) \leq 1 \, \forall \, V_G. \tag{8}$$

It is, therefore, possible to obtain an average value of k by simply fitting $\left(\frac{d\sqrt{I}}{dV_G}\right)^2$ with a power law function and using the extracted value of β to calculate k (supplementary material, Sec. 4, Ref. 29). Although a power law is used to extract the correction factor, this method gives the possibility to extract the value of the gate voltage dependent mobility without forcing any *a priori* explicit functional dependence. The consistency of the results is shown by its agreement with the second derivative method (Figure S1, supplementary material, Ref. 29). The standard saturation mobility equation which neglects this correction factor will lead to an underestimation of the gate voltage dependent mobility.[34]

This article is copyrighted as indicated in the article. Reuse of AIP content is subject to the terms at: http://scitation.aip.org/termsconditions. Downloaded to IP: 141.89.117.114 On: Thu, 17 Jul 2014 14:35:01

The actual value of the onset voltage[9] can be easily estimated *a posteriori* from the $\mu(V_G)$ curve, as the voltage at which the mobility rises above the noise level.

The accurate estimation of the charge density dependent mobility in the saturation regime allows determining the actual potential drop along the channel from the first derivative of the current against the gate voltage in the linear regime of operation ($V_D \ll V_G$)

$$\frac{dI}{dV_G} \cong \frac{W}{L} C_i \mu(V_G) V_{D^*S^*}, \tag{9}$$

where all the terms containing $\frac{dV_{D^*S^*}}{dV_G}$ are neglected, and only the first term of the Taylor series expansion is considered (supplementary material, Sec. 3, Ref. 29).

Under the above mentioned conditions, the quantity $\mu(V_G)$ appearing in Eqs. (5) and (9) is the same one. It is, therefore, straightforward to obtain the channel voltage $V_{D^*S^*}$ from the ratio of Eq. (9) and Eq. (6)

$$\frac{\frac{dI_{lin}}{dV_G} \cdot k}{2\left(\frac{d\sqrt{I_{sat}}}{dV_G}\right)^2} \cong V_{D^*S^*}(V_G). \tag{10}$$

Knowing the voltage drop along the channel, it is possible to estimate the total contact resistance $R_C = R_S + R_D$ by simply dividing the voltage drop at the contacts by the measured current, without assuming any specific dependence on the gate voltage

$$R_C(V_G, V_{DS}) = \frac{(V_{DS} - V_{D^*S^*}(V_G))}{I_d^{lin}}, \tag{11}$$

where the dependence of R_C on V_G and V_{DS} is evident. The possibility of extracting $R_C(V_G, V_{DS})$ and charge density dependent $\mu(V_G)$ for any transistor geometry and without requiring any additional measurement makes this approach extremely versatile. Equation (4) is the only extra assumption required in order for the model to provide consistent results.

When comparing results obtained from the analysis of output and transfer curves, one has to note that the former leads to the determination of the effective mobility, as shown here in the case of no contact resistance

$$\left.\frac{dI}{dV_D}\right|_{V_D \to 0} = \frac{W}{L} C_i \cdot V_G \cdot \mu_{eff}(V_G), \tag{12}$$

so that Eq. (2) is required in order to compare the obtained values.

The validity of this model is now assessed by preparing FPP field-effect transistors and a set of different channel length transistors for gated-TLM characterization, where experimental and analytical extraction methods can be compared on the very same device using the same set of measurements. All devices were prepared on photolithographically defined gold source-drain electrodes on glass substrates, using either poly[2,5-bis(3-tetradecylthiophen-2-yl)thieno[3,2-b]thiophene] (pBTTT)[35] or poly{[N,N′-bis(2-octyldodecyl)-naphthalene-1,4,5,8-bis(dicarboximide)-2,6-diyl]-alt-5,5′-(2,2′-bithiophene)} (P(NDI2OD-T2)[36] as semiconducting layer, poly(methylmethacrylate) (PMMA, $\varepsilon_r = 3.6$) as dielectric layer, and aluminum as gate electrode (full details on device preparation and geometry are available in the supplementary material, Sec. 5, Ref. 29).

In Figures 2(a) and 2(b), the charge density dependent mobility extracted from the FPP measurement in the linear regime (using the linear extrapolation of the channel potential[20] together with Eq. (9)) is compared with the mobility extracted from the saturation transfer characteristics using Eq. (6). In the case of pBTTT, the agreement between the two methods is particularly good for $V_{DS} = -10$ V, while the experimental curve for $V_{DS} = -5$ V suffers from a slightly offset voltage measured on the voltage probe close to the source. The agreement is slightly less good for P(NDI2OD-T2), with the mobility extracted from Eq. (6) underestimating the value obtained from the FPP measurements at low gate voltages (supplementary material, Sec. 6, Ref. 29).

In Figures 2(c) and 2(d), the extracted value for the contact resistance is shown both for the FPP measurements and using Eq. (11), the latter demonstrating how the analytical method recovers the full dependence of R_C on both V_{DS} and V_{GS}. For the pBTTT device, the agreement is very good through the whole range (the traces overlap for most of the graphs), with the exception of the experimental measurement at $V_{DS} = -5$ V which again suffers from the offset on the voltage measured on the source probe (hence the drop in the measured contact resistance). Also for P(NDI2OD-T2) (Figure 2(d)), the agreement with the experimental data is particularly good at high gate voltages ($V_G \geq 20$ V). At low

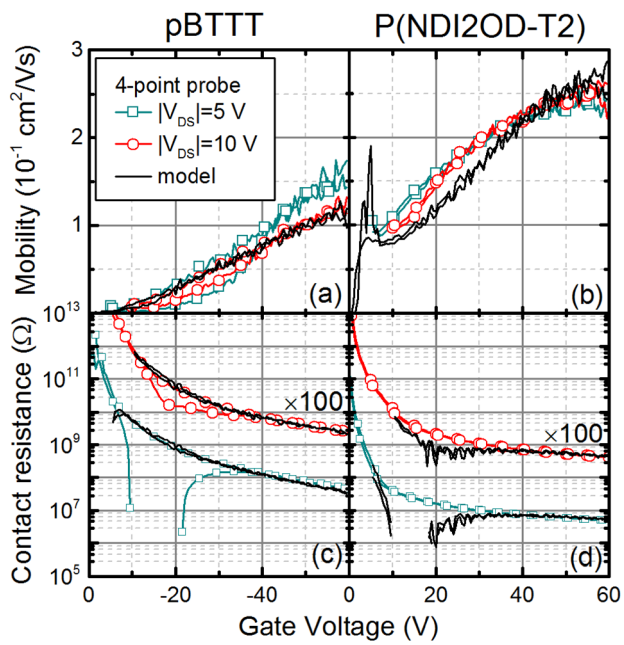

FIG. 2. Comparison of the mobility extracted from the four point probe measurement (lines + symbols) for $|V_{DS}| = 5$ V and $|V_{DS}| = 10$ V, positive for P(NDI2OD-T2) and negative for pBTTT and the charge density dependent mobility extracted from the transfer characteristics of a single transistor using Eq. (6) (black line) for p-type (a) (pBTTT) and n-type (b) (P(NDI2OD-T2). (c) and (d) Comparison of the contact resistance extracted with the four point probe (lines + symbols) and our model (black line), for pBTTT and P(NDI2OD-T2), respectively. Curves for $|V_{DS}| = 10$ V are offset by two orders of magnitude for clarity.

This article is copyrighted as indicated in the article. Reuse of AIP content is subject to the terms at: http://scitation.aip.org/termsconditions. Downloaded to IP: 141.89.117.114 On: Thu, 17 Jul 2014 14:35:01

gate voltages, the saturation mobility becomes equal or lower than the linear one (Figure S3, supplementary material, Ref. 29) leading to a negative contact resistance, which might be related to the condition in Eq. (4) not being met for this device at low gate voltages, probably due to some degradation occurring during the patterning process (the P(NDI2OD-T2) devices used for TLM characterization do not show this effect).[37]

The main limiting factor determining the uncertainty in the calculated parameters is the accuracy of the measurement setup (the relative error on current measurement for the measurement setup is $\xi_i \cong 10^{-3}$), since the uncertainty in the estimation of channel dimensions and capacitance will have the same impact on calculated and measured values, canceling out when comparing the results. Taking into account the numerical derivation, the final accuracy ξ_C is usually between 3% and 10% for both mobility and contact resistance (a detailed analysis of the uncertainty for the FPP measurement is reported in the supplementary material, Sec. 7, Ref. 29). While at low voltages the differences between measured and calculated values are significant for the reasons explained in the previous paragraph, at high gate voltages, the difference between calculated and measured parameters is always lower than $2 \cdot \xi_C$, with the proposed method extracting values that are in full agreement with the ones obtained by direct experimental methods.

We performed a similar comparison with the TLM.[38] The total resistance for a set of P(NDI2OD-T2) transistors against different channel lengths, extracted for different gate voltages from the slope of the output curve between $V_{DS} = 1\,\text{V}$ and $V_{DS} = 4\,\text{V}$ (supplementary material, Sec. 8, Ref. 29), has been fitted with a straight line according to the standard TLM equation (note the use of the effective mobility, according to Eq. (12))[39]

$$R_D = R_C + \frac{L}{WC_i(V_G - V_{on})\mu_{eff}}. \tag{13}$$

Figures 3(a) and 3(b) show contact resistance and charge density dependent mobility, respectively, extracted from the TLM measurements and using the analytical model for devices with 5 μm and 12 μm channel length. As can be seen, the contact resistance extracted from the analytical method has the same gate voltage dependence as the values extracted from the TLM analysis. The different gate voltage dependence of contact resistance compared to the 4 point probe devices (Figure 2) is due to the much larger overlap between the gate and source-drain electrodes in the TLM devices, leading to a much longer effective contact length. The contact resistance extracted for the 5 μm channel device is slightly lower than for the 12 μm one, which is probably due to device to device variation. In Figure 3(b), the mobility extracted by the two methods are compared, showing how the mobility extracted from the TLM analysis correctly matches with the effective mobility (calculated using Eq. (2)).

In Figure 4, the developed model is used to study the dependence of contact resistivity on the thickness of the semiconducting layer (at $V_G = 58\,\text{V}$) for two sets of P(NDI2OD-T2) transistors with different preparation

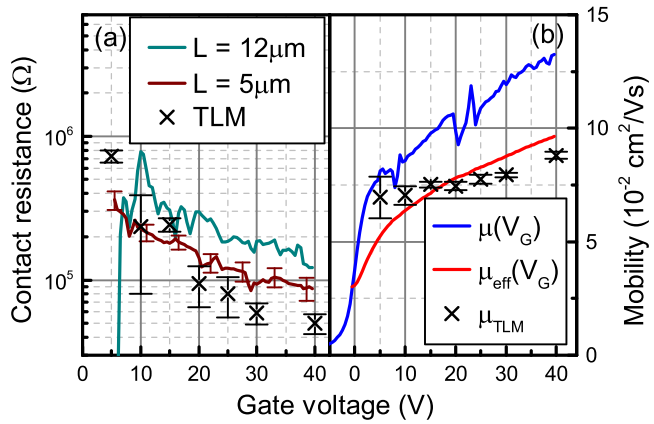

FIG. 3. (a) Comparison of the contact resistance of P(NDI2OD-T2) transistors extracted with the TLM and with our model for the transistors with channel length of 5 μm and 12 μm. Error bars, shown only for the 5 μm channel for clarity, are similar for the 12 μm channel length. (b) Comparison of the mobility extracted from the slope of the TLM plots and the charge density dependent and effective field-effect mobility calculated using the analytical model for the 5 μm channel transistor.

conditions (a scenario where TLM measurement would be unpractical for the high number of devices required and four point probe would be complicated by the thickness of some of the measured devices). We compared a set of devices prepared using chlorobenzene (CB), a solvent that promotes strong aggregation in the polymer film and produces films with high electron mobility (~0.2 cm^2/Vs) and a face-on orientation of the polymer chains with respect to the substrate, with a set of devices prepared using a 1:1 mixture of chloronaphthalene:xylene (CN:Xyl), which inhibits aggregation, leading to films with lower charge carrier mobility (~0.06 cm^2/Vs) and edge-on orientation of the polymer chains.[40,41] Contact resistivity was obtained from the contact resistance values using the current crowding model proposed by Chiang *et al.*[18] As expected from the different device preparation conditions, for large thicknesses, there is a clear difference in contact resistivity due to the higher bulk resistivity of the CN:Xyl films. However, for film thicknesses of roughly 40 nm, contact resistance of both films becomes

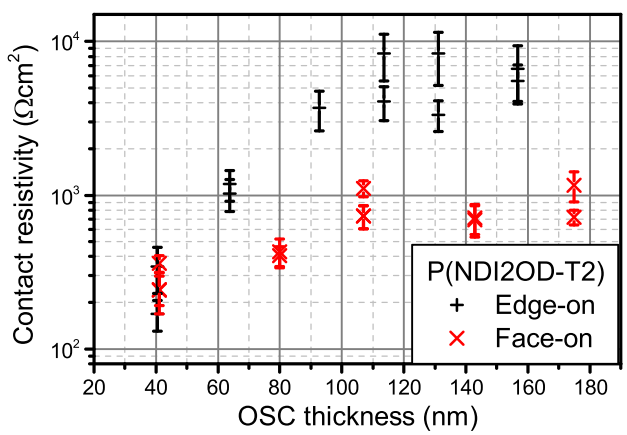

FIG. 4. Contact resistivity at $V_G = 58\,\text{V}$ for P(NDI2OD-T2) transistors with different thicknesses of the organic semiconductor layer, showing the influence of the increased bulk resistance on contact resistivity. The difference in bulk conductivity between face-on and edge-on polymer chains is lost for thinner films, suggesting an altogether different morphology on top of the gold source drain electrodes.

This article is copyrighted as indicated in the article. Reuse of AIP content is subject to the terms at: http://scitation.aip.org/termsconditions. Downloaded to IP: 141.89.117.114 On: Thu, 17 Jul 2014 14:35:01

comparable, therefore, suggesting an altogether different film morphology on top of the gold source and drain electrodes which extends for more than 10 nm in the bulk. The origin of this behavior is currently under investigation.

In conclusion, a very simple and compact model is proposed for the extraction of charge density dependent mobility and variable contact resistance which can be easily applied to any transistor geometry. It allows extracting accurate values for both charge density dependent mobility and gate voltage dependent contact resistance, completely separating the contribution of each parameter to the total current without any *a priori* assumption or the analysis of multiple devices. By taking into account both variable contact resistance and charge density dependent mobility, it solves all the inconsistencies between the mobility extracted from the transfer characteristics and from the output curves, providing an accurate estimation of the carrier mobility. As such, this model can be a valuable tool to characterize charge-transport mechanisms and charge-carrier injection in field-effect transistors, with potential applications in the analysis of the charge-transfer processes at the metal-organic semiconductor interface.

This work was financially supported by the Deutsche Forschungsgemeinschaft (DFG) within the Collaborative Research Centre HIOS (SFB 951). A.K. and E.L.-K. gratefully acknowledge the financial support of the Styrian Government (project BioOFET 2, GZ:A3-11.B-36/2010-5). R.D.P. would like to thank Mr. Daniel Pinkal for useful discussion during the preparation of the manuscript.

[1]R. A. Street, Adv. Mater. **21**, 2007 (2009).
[2]C. D. Dimitrakopoulos and D. J. Mascaro, IBM J. Res. Dev. **45**, 11 (2001).
[3]S. M. Sze, *Semiconductor Devices: Physics and Technology* (Wiley, 1985), p. 523.
[4]M. C. J. M. Vissenberg and M. Matters, Phys. Rev. B **57**, 12964 (1998).
[5]G. Horowitz, P. Lang, M. Mottaghi, and H. Aubin, Adv. Funct. Mater. **14**, 1069 (2004).
[6]G. Ghibaudo, Electron. Lett. **24**, 543 (1988).
[7]Y. Xu, T. Minari, K. Tsukagoshi, J. A. Chroboczek, and G. Ghibaudo, J. Appl. Phys. **107**, 114507 (2010).
[8]S. Jain, IEE Proc. **135**(6), 162–165 (1988).
[9]C. Reese and Z. Bao, J. Appl. Phys. **105**, 024506 (2009).
[10]M. Gruber, E. Zojer, F. Schürrer, and K. Zojer, Adv. Funct. Mater. **23**, 2941 (2013).
[11]B. Hamadani, H. Ding, Y. Gao, and D. Natelson, Phys. Rev. B **72**, 235302 (2005).
[12]D. Natali and M. Caironi, Adv. Mater. **24**, 1357 (2012).
[13]G. K. Reeves and H. B. Harrison, IEEE Electron Device Lett. **3**, 111 (1982).
[14]Y. Xu, R. Gwoziecki, I. Chartier, R. Coppard, F. Balestra, and G. Ghibaudo, Appl. Phys. Lett. **97**, 063302 (2010).
[15]J. Zaumseil, K. W. Baldwin, and J. A. Rogers, J. Appl. Phys. **93**, 6117 (2003).
[16]E. J. Meijer, G. H. Gelinck, E. van Veenendaal, B.-H. Huisman, D. M. de Leeuw, and T. M. Klapwijk, Appl. Phys. Lett. **82**, 4576 (2003).
[17]H. Sirringhaus, N. Tessler, D. S. Thomas, P. J. Brown, and R. H. Friend, Adv. Solid State Phys. **39**, 101 (1999).
[18]C. Chiang, S. Martin, J. Kanicki, Y. Ugai, T. Yukawa, and S. Takeuchi, Jpn. J. Appl. Phys., Part 1 **37**, 5914 (1998).
[19]S. Gamerith, A. Klug, H. Scheiber, U. Scherf, E. Moderegger, and E. J. W. List, Adv. Funct. Mater. **17**, 3111 (2007).
[20]P. V. Pesavento, K. P. Puntambekar, C. D. Frisbie, J. C. McKeen, and P. P. Ruden, J. Appl. Phys. **99**, 094504 (2006).
[21]T. J. Richards and H. Sirringhaus, J. Appl. Phys. **102**, 094510 (2007).
[22]M. Caironi, M. Bird, D. Fazzi, Z. Chen, R. Di Pietro, C. Newman, A. Facchetti, and H. Sirringhaus, Adv. Funct. Mater. **21**, 3371 (2011).
[23]K. Seshadri and C. D. Frisbie, Appl. Phys. Lett. **78**, 993 (2001).
[24]L. Bürgi, T. J. Richards, R. H. Friend, and H. Sirringhaus, J. Appl. Phys. **94**, 6129 (2003).
[25]R. A. Street and A. Salleo, Appl. Phys. Lett. **81**, 2887 (2002).
[26]P. V. Necliudov, M. S. Shur, D. J. Gundlach, and T. N. Jackson, J. Appl. Phys. **88**, 6594 (2000).
[27]D. Natali, L. Fumagalli, and M. Sampietro, J. Appl. Phys. **101**, 014501 (2007).
[28]G. Horowitz, R. Hajlaoui, D. Fichou, and A. El Kassmi, J. Appl. Phys. **85**, 3202 (1999).
[29]See supplementary material at http://dx.doi.org/10.1063/1.4876057 for the full mathematical derivation of the transistor equation and additional experimental details.
[30]S. M. Sze and K. K. Ng, *Physics of Semiconductor Devices* (John Wiley and Sons, New Jersey, 2007).
[31]G. Lu, J. C. Blakesley, S. Himmelberger, P. Pingel, J. Frisch, I. Lieberwirth, I. Salzmann, M. Oehzelt, R. Di Pietro, A. Salleo, N. Koch, and D. Neher, Nat. Commun. **4**, 1588 (2013).
[32]L. Bürgi, T. Richards, M. Chiesa, R. H. Friend, and H. Sirringhaus, Synth. Met. **146**, 297 (2004).
[33]H. Baüssler and A. Köhler, Top. Curr. Chem. **312**, 1 (2012).
[34]H. Klauk, Chem. Soc. Rev. **39**, 2643 (2010).
[35]I. McCulloch, M. Heeney, C. Bailey, K. Genevicius, I. Macdonald, M. Shkunov, D. Sparrowe, S. Tierney, R. Wagner, W. Zhang, M. L. Chabinyc, R. J. Kline, M. D. McGehee, and M. F. Toney, Nature Mater. **5**, 328 (2006).
[36]H. Yan, Z. Chen, Y. Zheng, C. Newman, J. R. Quinn, F. Dötz, M. Kastler, and A. Facchetti, Nature **457**, 679 (2009).
[37]R. Di Pietro, D. Fazzi, T. B. Kehoe, and H. Sirringhaus, J. Am. Chem. Soc. **134**, 14877 (2012).
[38]A. Klug, A. Meingast, G. Wurzinger, A. Blümel, K. Schmoltner, U. Scherf, and E. J. W. List, Proc. SPIE **8118**, 811809 (2011).
[39]M. Kano, T. Minari, and K. Tsukagoshi, Appl. Phys. Lett. **94**, 143304 (2009).
[40]S. Fabiano, H. Yoshida, Z. Chen, A. Facchetti, and M. A. Loi, ACS Appl. Mater. Interfaces **5**, 4417 (2013).
[41]R. Steyrleuthner, R. Di Pietro, B. A. Collins, F. Polzer, S. Himmelberger, M. Schubert, Z. Chen, S. Zhang, A. Salleo, H. W. Ade, A. Facchetti, and D. Neher, J. Am. Chem. Soc. **136**, 4245 (2014).

This article is copyrighted as indicated in the article. Reuse of AIP content is subject to the terms at: http://scitation.aip.org/termsconditions. Downloaded to IP: 141.89.117.114 On: Thu, 17 Jul 2014 14:35:01